

Flow resistance equations for mountain rivers

R. López Alonso^{1*}, J. Barragán Fernández¹ and M.^a À. Colomer Cugat²

¹ *Department of Agroforestry Engineering, University of Lleida. Av. Alcalde Rovira Roure, 191. E25198 Lleida, Spain.*

² *Department of Mathematical, University of Lleida. C/ Jaume II, 69, Campus Cappedon, E25001, Lleida, Spain.*

Abstract

Three models of flow resistance (a Keulegan-type logarithmic law and two models developed for large-scale roughness conditions: the full logarithmic law and a model based on an inflectional velocity profile) were calibrated, validated and compared using an extensive database ($N = 1,533$) from rivers and flumes, representative of a wide hydraulic and geomorphologic range in the field of gravel-bed and mountain channels. It is preferable to apply the model based on an inflectional velocity profile in the relative submergence (y/d_{90}) interval between 0.5 and 15, while the full logarithmic law is preferable for values below 0.5. For high relative submergence, above 15, either the logarithmic law or the full logarithmic law can be applied. The models fitted to the coarser percentiles are preferable to those fitted to the median diameter, owing to the higher explanatory power achieved by setting a model, the smaller difference in the goodness-of-fit between the different models and the lower influence of the origin of the data (river or flume).

Key words: friction factor; grain-size percentile; high-gradient streams; cross validation.

Resumen

Ecuaciones de resistencia al flujo para ríos de montaña

Se han calibrado, validado y comparado tres modelos de resistencia al flujo (una ley logarítmica tipo Keulegan y dos modelos desarrollados para condiciones de alta rugosidad: la ley logarítmica completa y un modelo basado en un perfil de velocidad inflexional) empleando para ello una extensa base de datos ($N = 1,533$) de río y de laboratorio, representativa de un amplio intervalo hidráulico y geomorfológico en el ámbito de cauces de grava y de montaña. El modelo basado en un perfil de velocidad inflexional es preferible para su aplicación en el intervalo de sumersión relativa (y/d_{90}) comprendido entre 0.5 y 15, mientras que la ley logarítmica completa es preferible para valores inferiores a 0.5. Para sumersión relativa alta, por encima de 15, es posible aplicar indistintamente la ley logarítmica y la ley logarítmica completa. Son preferibles los modelos ajustados con los percentiles más gruesos que los ajustados con el diámetro mediano, debido a: la mayor capacidad explicativa alcanzada fijado un modelo, la menor diferencia en la bondad de ajuste entre los diferentes modelos y la menor influencia del origen de los datos (río o laboratorio).

Palabras clave: factor de fricción; percentil granulométrico; cauces de fuerte pendiente; validación cruzada.

Introduction

Fluvial hydraulics must search for the solution to the problems related to prediction or determination of the relationship between flow discharge (or its mean velocity) and hydraulic geometry; the sediment transport capacity of the flow; the erosion and sedimentation at the reach scale and the general dynamics of the fluvial geomorphology. These applications make up a scale,

that is, each of the more complex levels includes all the problems from the simpler levels, so that the last one must solve the previous ones. Consequently, in all of these it is necessary to determine the resistance of the channel to the flow, bearing in mind that this process corresponds to the first of the above-mentioned problems.

Until a few decades ago, those problems associated with coarse material-bed rivers (gravel, cobble or boul-

* Corresponding author: rlopez@aegrof.udl.cat

Received: 22-10-08. Accepted: 18-02-09.

der size) were not preferably studied, as this type of river was frequently found in less populated, higher and more peripheral regions, which, combined with the greater complexity of the hydro-geomorphologic processes that are found in these, meant that they were traditionally less well known than the alluvial plain sand-bed rivers. In contrast with the latter, mountain coarse material-bed rivers are characterized by channels with a greater longitudinal gradient, larger size and more heterogeneous sediment, greater connection with the slope morphogenetic processes, greater relevance of bed load transport, flow with smaller relative submergence and different bed forms. This article is designed to contribute to improving our ability to predict the flow resistance in coarse material-bed rivers.

For steady and uniform open channel flow, the cross-sectional average velocity V may be expressed with the Darcy-Weisbach equation as

$$\sqrt{8/f} = V / v_* \quad (1)$$

where f = Darcy-Weisbach friction factor, and v_* = shear velocity. The shear velocity can be estimated as $v_* = \sqrt{gRS}$, where g = gravitational acceleration, R = cross-sectional hydraulic radius, and S = bed slope. If we consider a channel composed of granular particles with a unidirectional, turbulent and hydraulically rough flow of which depth is much larger than the size of these particles and, moreover, it is accepted that the vertical velocity profile is logarithmic, a Keulegan-type equation can be obtained

$$\frac{V}{v_*} = \frac{2.303}{\kappa} \log\left(\frac{h}{z_0}\right) + B \quad (2)$$

where V = mean velocity on the vertical plane analysed, κ = von Karman coefficient, h = depth in this plane, B = coefficient and z_0 = hydraulic roughness of the boundary. The hydraulic roughness of the boundary, which represents the distance from the bed at which the logarithmic distribution is zero, can be related linearly to the equivalent roughness k_s (i.e., $z_0 \propto k_s$). This in turn, can be replaced by a linear relation with a characteristic particle diameter d_i (i.e., $k_s \propto d_i$). If two-dimensional flow is assumed, the vertical velocity profile will not be affected by the presence of the banks, thus V in Eq. (2) would represent the cross-sectional mean velocity and it would be acceptable to replace h with the mean flow depth y . As a result of the above considerations and if, moreover, κ is accepted as a parameter susceptible to fitting (e.g., Aberle and Smart, 2003), equation (2) can finally be written as

$$\sqrt{\frac{8}{f}} = A_1 \log\left(\frac{y}{d_i}\right) + A_2 \quad (3)$$

where A_1 and A_2 are the coefficients. If all particles are completely submerged, but z_0 is not negligible with respect to h (i.e., when the flow relative submergence y/d_i is low), under the same conditions stated for Eq. (3) the full logarithmic equation is (Smart *et al.*, 2002)

$$\sqrt{\frac{8}{f}} = B_1 \left(\left(\frac{y}{y - B_2 d_i} \right) \ln \left(\frac{y}{B_2 d_i} \right) - 1 \right) \quad (4)$$

where B_1 and B_2 are the coefficients.

Also for flow under high relative roughness conditions, Katul *et al.* (2002) propose an inflectional velocity profile divided into two zones: a lower one that corresponds to flow just under the mean height of the roughness elements, at low velocity and more homogeneous, and another situated above the previous one, with a steeper gradient and higher velocity. After integrating this distribution, and imposing conditions that are analogous to those adopted for equations (3) and (4) we obtain

$$\sqrt{\frac{8}{f}} = C_1 \left(1 + \frac{C_2 d_i}{y} \ln \left(\frac{\cosh \left(\frac{1}{C_2} - \frac{y}{C_2 d_i} \right)}{\cosh(1/C_2)} \right) \right) \quad (5)$$

where C_1 and C_2 are the coefficients. C_1 is the so-called similarity coefficient and C_2 is a coefficient of proportionality between the characteristic turbulent eddy size and d_i . According to Katul *et al.* (2002), $C_2 \approx < 1.0$ and, if $d_i = d_{84}$ is imposed, C_1 is equal to approximately 5.8 for high submergence flow and takes on lower values for high relative roughness. When $C_2 \gg 1.0$, as might occur in a mobile bed, the proposed velocity distribution might not be valid. As a first approximation, $C_1 = 4.5$ is recommended for low submergence flow in gravel-bed rivers and, if we accept that the characteristic turbulent eddy size is of the order of the characteristic diameter size, then $C_2 = 1.0$. The graphic evaluation of the goodness-of-fit of the proposed model with respect to a set of data from rivers and flumes, using the above-mentioned values as parameters leads the mentioned authors to consider that the model yields satisfactory results for values of y/d_{84} between 0.2 and 7.0.

Table 1 shows a selection of values for the coefficients of models (3), (4) and (5), proposed in previous research into coarse material-bed rivers, with the aim of comparing these with the values obtained in this study. Among other causes, the variability shown in this table

Table 1. Selection of coefficient values determined by different researchers in coarse material-bed channels

| Model | Reference | d_i | Coefficients | N_c | Observations |
|-------|----------------------------|----------|----------------------------|-------|--------------------------------|
| (3) | Griffiths (1981) | d_{50} | $A_1 = 5.60; A_2 = 2.15$ | 186 | Gravel-bed rivers. |
| (3) | Ugarte and Méndez (1994) | d_{50} | $A_1 = 4.63; A_2 = 2.50$ | 168 | Coarse material-bed rivers. |
| (3) | Bathurst (1985) | d_{84} | $A_1 = 5.62; A_2 = 4.00$ | 44 | Coarse material-bed rivers. |
| (3) | Knighton (1998) | d_{84} | $A_1 = 5.34; A_2 = 3.41$ | 162 | Gravel-bed rivers. |
| (3) | Ferguson (2007) | d_{84} | $A_1 = 5.76^a; A_2 = 2.53$ | 376 | Gravel and boulder-bed rivers. |
| (3) | Bray (1979) | d_{90} | $A_1 = 6.11; A_2 = 3.56$ | 67 | Gravel-bed rivers. |
| (3) | Maynard (1991) | d_{90} | $A_1 = 3.92; A_2 = 6.86$ | 95 | Riprap flumes. |
| (4) | Smart <i>et al.</i> (2002) | d_{84} | $B_1 = 2.50^a; B_2 = 0.10$ | 88 | Flume data with fixed bed. |
| (4) | López <i>et al.</i> (2006) | d_{90} | $B_1 = 3.43; B_2 = 0.12$ | 236 | Riprap channels. |
| (5) | Katul <i>et al.</i> (2002) | d_{84} | $C_1 = 4.50; C_2 = 1.00$ | 100 | Flumes and gravel-bed rivers. |
| (5) | López <i>et al.</i> (2006) | d_{90} | $C_1 = 6.47; C_2 = 1.22$ | 236 | Riprap channels. |

N_c = number of calibration data.

^aFixed value.

may be due to the differences in the experimental database of calibration, such as the origins of the data (river or flume), the heterogeneity of the sediment (both the size and shape of the particles as well as their disposition), the variability in the bed forms (at both a small and large scale (e.g., pool-riffle, step-pool, cascade)), or the intensity and mode of sediment transport. Nor should we underestimate the differences in the methods for obtaining data from coarse material-bed rivers.

With regard to the influence of the grain size percentile, different authors find that when flow resistance models are fitted expressing the relative submergence as a function of the coarser percentiles of the sediment sample, greater explanatory power is achieved than when these are fitted to the median diameter. This is attributed to different causes: the energy loss provoked by the coarser particles is more than proportional to their size (e.g., Prestegard, 1983; Van Rijn, 1982; Whiting and Dietrich, 1990); these particles reproduce the effect of the microtopographic bedforms on the energy loss more satisfactorily (Clifford *et al.*, 1992); the largest percentiles are more sensitive and representative of the concentration of coarser elements in the context of poorly sorted beds (Ferro and Giordano, 1991); and the coarser percentiles (roughly between d_{65} and d_{90}) show more precision of sampling than the median diameter d_{50} when the particle-size distribution is characterised with the Wolman method (e.g., Green (2003); Rice and Church (1996)).

This article aims to calibrate and validate a set of models for predicting the friction factor in coarse material bed rivers, using a large database representative of a wide range of hydraulic and geomorphological conditions in the context of gravel-bed rivers and mountain streams. At the

same time, it attempts to analyse the effect of the explicit consideration in the theoretical development of high relative roughness conditions on the models' explanatory power. In other words, whether models (4) and (5) behave better than model (3). Moreover, the influence of the grain-size percentile on the explanatory power of the fitted models is analysed with the purpose of checking whether this power increases for the coarser percentiles. Finally, the influence of the empirical origin of the data (i.e., river or flume) on the fitted models is studied.

Material and Methods

The criteria adopted for compiling the calibration and validation database is explained below. The channel reach, whether a river or a flume, must correspond to a single straight channel, with a steady, uniform, in-bank flow. It must be free of vegetation and natural or artificial obstacles. These conditions allow us to assume that the effects of vegetation and changes in the channel shape (cross section, slope and alignment) on the flow resistance are minimal. However, it is necessary to keep in mind that, owing to the morphology of mountain and gravel-bed rivers and the low relative submergence, flow is in fact varied at a detailed scale. Thus, the requirement of uniformity must be understood as an average along a stretch. In other words, it is enough to consider that the flow is macroscopically uniform.

Moreover, the sediment must be gravel, cobble or boulder size, explicitly excluding channels with cohesive sediment, sand or rock beds. To this end, it is assumed that the value of d_{50} must be greater than or

equal to 2 mm. Similarly, the flow must be turbulent (Reynolds number Re above 2,000) and hydraulically rough (grain shear Reynolds number Re_* above 200). The two numbers were calculated, respectively, as $Re = V \cdot R/\nu$ and $Re_* = v_* \cdot d_{50} / \nu$, where ν = kinematic viscosity of water. For rivers, with the aim of ensuring that the flow in the central zone of the cross section is not influenced by the channel banks, the ratio of free surface width T to mean depth y must be higher than approximately 10 (which implies that $R \approx y$). In contrast, for flume data, the application of one of the habitual wall drag correction methods is considered sufficient. The method used in this research is described in Smart (1984). Various bibliographic sources consulted provide data for different river reaches for which, in turn, data has been obtained for different discharges. Despite meeting the requisites imposed, anomalous behaviour has been observed on occasions in all or part of the data for a reach (e.g., outliers or an abnormal trend of flow resistance with relative submergence). In this case, it was decided to adopt the criteria of rejecting all the data from the reach in question, but still accepting data obtained in other valid reaches in the same source.

Applying the selection requirements stated above yielded a set that includes 1,533 data from rivers and flumes, corresponding to 42 bibliographic references from 1955 to 2003 and also to our own research in rivers on the Spanish slopes of the Pyrenees (López, 2005). This database is among the largest that has ever been used to fit flow resistance equations in coarse material-bed rivers and high-gradient streams. If the size and variety of the database compiled is taken into account, the number of sources consulted, the period these cover

and the measurement conditions in mountain rivers, it is impossible to guarantee rigorous uniformity in either the measurement procedures or the uniform quality of the data. However, the type of variables measured (mean flow velocity or discharge, depth, longitude and grain size) and the similarity of the methods used, means that there can be considered to be a high enough degree of uniformity for the aims proposed.

Table 2 shows the maximum, minimum and mean values and the coefficient of variation (C_v) of the main adimensional variables, for both the full data set, and separately for the river and flume subsets. The database is representative of a wide hydraulic and geomorphologic interval in the context of coarse material bed rivers. The relative submergence varies by three orders of magnitude and the slope, by four. If the river and flume subsets are compared it can be deduced that, although the mean relative submergence of both is similar, the river subset extends over a wider interval, which is the result of including bankfull level data. On the other hand, the flume subset has a higher mean slope (almost triple) than the river subset, although the latter includes a wider interval. Among the consequences of the significantly higher slope in the laboratory flumes is a greater representation of mobile bed conditions in the flume subset than in the river data. In fact, for the great majority of the river data, no bedload transport was detected, while this mode of transport was found in 48% of the flume data. Among these, however, only in 26% did the value of the sediment mobility index τ/τ_c (where τ = mean shear stress; and τ_c = critical shear stress) correspond to intensive transport (i.e., $\tau/\tau_c > \approx 3$). In any case, the data correspond only to conditions

Table 2. Range of hydraulic variables in calibration database and river and laboratory databases

| Parameter | Symbol | | Minimum | Maximum | Mean | C_v (%) |
|---|--------------|-----|---------------------|---------------------|----------------------|-----------|
| <i>Calibration Database (N = 1,533)</i> | | | | | | |
| Friction factor | $\sqrt{8/f}$ | (-) | 0.13 | 20.6 | 7.3 | 49 |
| Relative submergence | y/d_{90} | (-) | 0.10 | 102.1 | 7.1 | 143 |
| Bed slope | S | (-) | $1.0 \cdot 10^{-5}$ | $2.0 \cdot 10^{-1}$ | $1.8 \cdot 10^{-2}$ | 147 |
| <i>River Database (N = 954)</i> | | | | | | |
| Friction factor | $\sqrt{8/f}$ | (-) | 0.13 | 20.6 | 6.7 | 55 |
| Relative submergence | y/d_{90} | (-) | 0.10 | 102.1 | 6.8 | 165 |
| Bed slope | S | (-) | $1.0 \cdot 10^{-5}$ | $1.6 \cdot 10^{-1}$ | $1.11 \cdot 10^{-2}$ | 147 |
| <i>Laboratory Database (N = 579)</i> | | | | | | |
| Friction factor | $\sqrt{8/f}$ | (-) | 1.29 | 17.0 | 8.4 | 39 |
| Relative submergence | y/d_{90} | (-) | 0.23 | 47.8 | 7.7 | 107 |
| Bed slope | S | (-) | $3.6 \cdot 10^{-4}$ | $2.0 \cdot 10^{-1}$ | $2.96 \cdot 10^{-2}$ | 119 |

with low concentrations of sediment transport, given that high concentrations of solid discharge can substantially modify the properties of the fluid and the flow, among these the flow resistance, so data that may correspond to a hyperconcentrated flow have been excluded.

In this study, the evaluation of models includes their calibration and validation, as well as a comparison between the models. The calibration consisted in fitting the parameters of the selected models to the entire database (i.e., $N = 1,533$) through the least-squares procedure. Each of the three models selected was fitted considering three grain-size percentiles (d_{90} , d_{84} and d_{50}), to analyse the influence of the characteristic diameter. To evaluate the goodness-of-fit of the models, the following were calculated: the coefficient of determination R^2 , the mean relative error MRE and the percentage of data with a relative error less than or equal to 25% RE_{25} and 50% RE_{50} . The MRE statistic is the mean percentage error between observation and prediction with regard to the observed value ($MRE = (100 / N) \sum |P_i - O_i| / O_i$, where O_i is the observed i value of the variable, P_i is the predicted i value of the variable and N is the number of data), so the error in each data contributes equally to the total value, independently of its magnitude. In a second phase, the models were validated by means of cross validation in the modality of test set switch (Esbensen *et al.*, 1994). To this end the models were fitted separately into two validation subsets (V_1 and V_2). These subsets were determined by randomly splitting the whole database (i.e., $N = 1,533$) that had been used previously for calibration into two parts, each made up of 50% of the total data. The final validation value of the statistics is the mean of the result of the cross validation of the equations fitted independently into both subsets. This is meant to avoid the loss of information in the calibration set that would occur with the test set validation (as this

would mean splitting the available database with the aim of assigning a part to calibration and another to validation). At the same time, thanks to the cross validation, a measure of the prediction error committed by the calibrated equations when they are applied to cases independently of the fit is also available.

Results

Table 3 shows the value of the fitted coefficients and the statistical indices for the models calibrated with the full database. From this table it follows that the goodness-of-fit of the equations that express the relative submergence as a function of d_{90} or d_{84} is higher than for the equation that includes d_{50} . Figure 1 shows the equations that appear in Tables 1 and 3 together. On the other hand, Table 3 shows that the difference in goodness-of-fit between the three models evaluated and for the same percentile is generally small. Nevertheless, if the goodness-of-fit of equations (8), (11) and (14) is compared, not globally, but rather by distinguishing different relative submergence intervals, relevant differences appear that allow one of them to be recommended over the others. In Figure 2, the three cited equations are represented along with the calibration database. Also in Figure 3, the $(8/f)^{1/2}$ values predicted by equations (8), (11) and (14) are plotted against the observed value.

Tables 4 and 5 show the value of the coefficients and the statistical indices corresponding, on the one hand, to the models fitted to the river database, and on the other, to those fitted to laboratory data, for the d_{50} and d_{90} grain-size percentiles respectively. Moreover, Figure 4 shows the equations that appear in Tables 4 and 5. Only these two grain-size percentiles (i.e., d_{50} and d_{90}) were selected so that the contrast between the results is as large as possible.

Table 3. Coefficients and statistics of the equations fitted to the calibration database ($N = 1,533$)

| Model | Eq. | Grain size | Coefficients | R^2 | MRE (%) | RE_{25} (%) | RE_{50} (%) |
|-------|------|------------|---------------------------|-------|---------|---------------|---------------|
| (3) | (6) | d_{50} | $A_1 = 5.36; A_2 = 2.87$ | 0.64 | 32 | 57 | 84 |
| (3) | (7) | d_{84} | $A_1 = 5.90; A_2 = 3.86$ | 0.75 | 25 | 67 | 88 |
| (3) | (8) | d_{90} | $A_1 = 5.85; A_2 = 4.20$ | 0.76 | 24 | 68 | 89 |
| (4) | (9) | d_{50} | $B_1 = 2.49; B_2 = 0.149$ | 0.64 | 34 | 57 | 83 |
| (4) | (10) | d_{84} | $B_1 = 2.83; B_2 = 0.124$ | 0.75 | 25 | 67 | 88 |
| (4) | (11) | d_{90} | $B_1 = 2.81; B_2 = 0.109$ | 0.76 | 23 | 67 | 89 |
| (5) | (12) | d_{50} | $C_1 = 5.19; C_2 = 2.75$ | 0.65 | 45 | 53 | 76 |
| (5) | (13) | d_{84} | $C_1 = 5.70; C_2 = 1.19$ | 0.74 | 27 | 69 | 88 |
| (5) | (14) | d_{90} | $C_1 = 5.87; C_2 = 1.25$ | 0.76 | 26 | 70 | 89 |

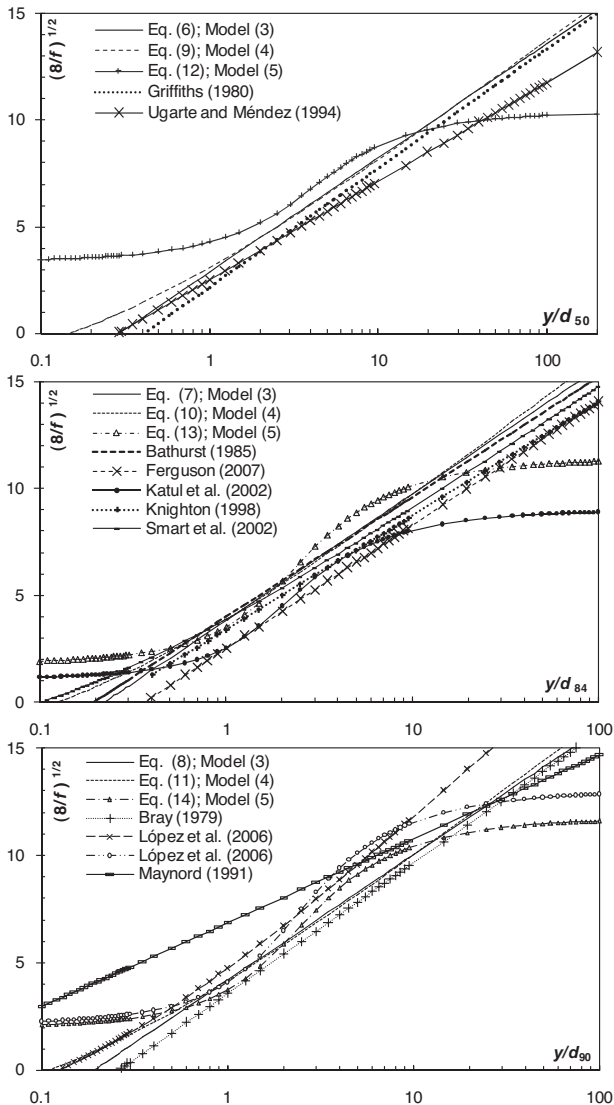


Figure 1. Representation of the equations from Tables 1 and 3.

The t test for mean differences and the F test for comparison of variances carried out on the two randomly generated validation subsets confirmed the similarity of both sets at a significance level of 0.05. The mean values of the statistical indices resulting from the crossed application of equations (8), (11) and (14), to both validation sets are shown in Table 6.

Discussion

From Table 3 it follows that the goodness-of-fit of the models that express the relative submergence as a function of coarser grain-size percentiles (d_{90} or d_{84}) is high-

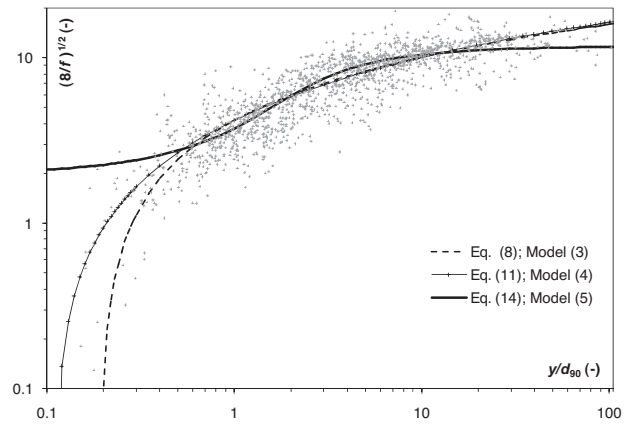


Figure 2. Representation of equations (8), (11) and (14) and the full calibration database.

er than for the model that includes median diameter (d_{50}). In terms of R^2 , the explanatory power of the equation fitted to d_{90} is, on average over the three models, 18% higher than that of the equation expressed as a function of d_{50} . Analogously, MRE was on average 33% lower in the three models, while RE_{25} and RE_{50} increased by 23% and 10% respectively. This coincides with other authors' findings for the logarithmic law (Burkham and Dawdy, 1976; Charlton *et al.*, 1978; Ferro and Giordano, 1991; Green, 2005; Limerinos, 1970; Ugarite and Méndez, 1994), the power law (Charlton *et al.*, 1978; López *et al.*, 2008; Maynard, 1991) or other laws for high relative roughness flow, such as those by Aguirre-Pe and Fuentes (1990) or Thompson and Campbell (1979) (López *et al.*, 2008). In the opposite sense, Bray (1979), using data from gravel and cobble-bed rivers with bankfull level, found no significant differences in the goodness-of-fit of the logarithmic laws and the power law in function of the grain-size percentile used (in his case d_{50} , d_{65} and d_{90}). The reason could lie in the predominance of data for high relative submergence, as these are for discharges corresponding to the bankfull level.

On the other hand, Table 3 shows that the difference in goodness-of-fit between the three models evaluated and for the same percentile is generally small. Thus, in overall terms and for the full set of data, better behaviour is not observed for the models whose theoretical development contemplated large-scale roughness conditions. However, the difference between the three models is greater if these have been fitted to d_{50} than if they have been fitted to d_{84} or d_{90} (see Figure 4). In fact, the mean variation in the value of the statistical indices

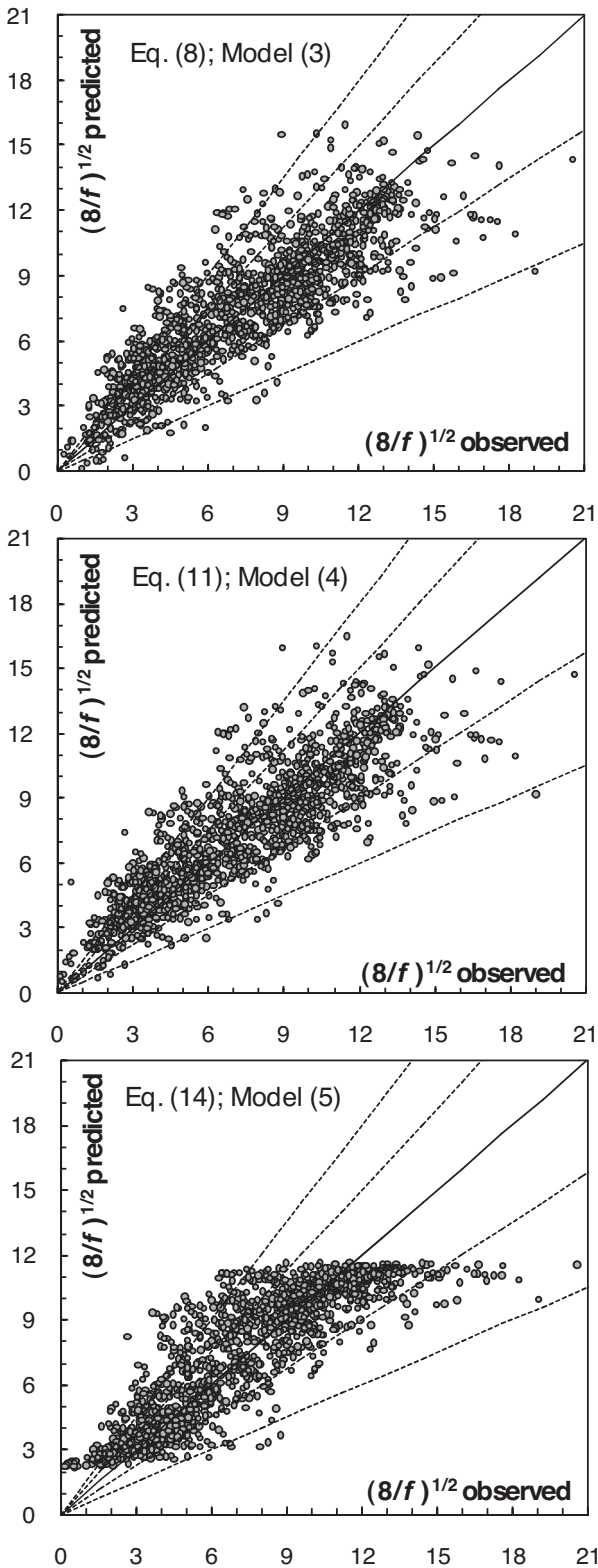


Figure 3. The $(8/f)^{1/2}$ predicted by equations (8), (11) and (14) plotted against the observed values. The lines corresponding to perfect agreement and $\pm 50\%$ and $\pm 25\%$ error are shown.

between the best and worse fitted equations is 12% for d_{50} and only 3% for d_{90} . It was also observed that model (5) is the most sensitive to the effect of the grain-size percentile, as it commits a considerably higher relative error than the other two for d_{50} , while the difference for d_{90} is much lower. In any case, it must be kept in mind that the differences observed between models upon setting a percentile are significantly lower than those detected for the same model when using d_{50} or d_{90} . Accordingly, it is preferable to apply models fitted to d_{90} rather than those fitted to d_{50} , which can also serve as a guide for future calibrations if only one percentile is used.

Nevertheless, if the goodness-of-fit of equations (8), (11) and (14) is compared, not globally, but rather by distinguishing different relative submergence intervals, relevant differences appear that allow one of them to be recommended over the others. From Figures 2 and 3 it can be seen that equations (8) and (11) generally follow similar trajectories, although they diverge in the region of lower relative submergence ($y/d_{90} \approx < 0.7$), where equation (11) achieves a better fit than equation (8). On the other hand, there are two important differences in equation (14) compared to the other two. First, it follows an inflectional trajectory that allows it to fit better to values of y/d_{90} in the 0.5–15 interval, as it adapts more flexibly to areas of higher density of dots. Secondly and in contrast, it has a poorer fit outside this interval, given that for values of y/d_{90} below 0.5, the dependent variable, $(8/f)^{1/2}$ tends asymptotically towards 2 and for values above 15, it tends towards 11 (see Figure 3). Thus, from the local analysis of the explanatory power, it is recommended to use equation (14) for its advantage over the other two, as long as its application is restricted to the stated interval (which coincides approximately with the recommendation made by Katul *et al.* (2002) to limit the application of model (5) to values of y/d_{84} in the interval 0.2–7). For y/d_{90} values below 0.5, the use of equation (11) is recommended, while for values above 15, either equations (8) or (11) can be used.

The value of coefficient A_1 for equations (6), (7) and (8) is very similar and corresponds to an average value of $\kappa = 0.40$, which coincides with the value that is typically considered universal. However, for equations (9), (10) and (11) B_1 has an average value that corresponds to $\kappa = 0.37$. Depending on the values of A_1 and A_2 in model (3) and the trajectories of the equations shown in the Figure 1, it could be concluded that the fitted equation by Griffiths (1981) is the closest to equation (6). Similarly, the equation by Bathurst (1985) is the one

Table 4. Coefficients and statistics of the models fitted separately to the river and flume databases. Grain-size percentile: d_{50} .

| Model | Eq. | Database | Coefficients | R^2 | MRE (%) | RE ₂₅ (%) | RE ₅₀ (%) |
|-------|------|----------|---------------------------|-------|---------|----------------------|----------------------|
| (3) | (15) | River | $A_1 = 5.35; A_2 = 2.09$ | 0.69 | 29 | 57 | 86 |
| (3) | (16) | Flume | $A_1 = 5.77; A_2 = 3.84$ | 0.74 | 19 | 78 | 91 |
| (4) | (17) | River | $B_1 = 2.39; B_2 = 0.181$ | 0.68 | 32 | 57 | 85 |
| (4) | (18) | Flume | $B_1 = 2.69; B_2 = 0.110$ | 0.74 | 19 | 78 | 91 |
| (5) | (19) | River | $C_1 = 4.94; C_2 = 4.34$ | 0.69 | 54 | 46 | 74 |
| (5) | (20) | Flume | $C_1 = 5.68; C_2 = 1.36$ | 0.73 | 21 | 78 | 89 |

that most closely resembles equation (7), given that the equation obtained by Ferguson (2007) predicts high flow resistance through having been fitted to a database with a high proportion of rivers with bedforms that provoke high energy losses (e.g., steep-pool or cascades). The equation by Bray (1979) describes a very similar trajectory to the one in equation (8), while the equation by Maynord (1991) predicts a much lower flow resistance for low relative submergence ($y/d_{90} < 20$), owing to the latter equation being fitted to data taken from riprap channels.

Depending on the value of B_1 and B_2 in model (4) and the trajectories of the equations represented in Figure 1, it can be stated that the equation proposed by Smart *et al.* (2002) resembles equation (10), while the one fitted by López *et al.* (2006) with data from riprap channels predicts lower flow resistance, except in very high relative roughness conditions.

The higher C_1 and C_2 values obtained for equations (12), (13) and (14), with respect to the theoretical value proposed by Katul *et al.* (2002) (i.e., $C_1 = 4.5; C_2 = 1.0$), could be attributed to the inclusion of an appreciable percentage of data with high relative submergence or corresponding to mobile bed conditions. To analyse the effect of this type of data, equation (5) was fitted again, but this time to a subset that only included 673 data items from rivers with submergence (y/d_{84}) ranging from 0.2 to 7. According to the characteristics of the

available database, in practice this implies fixed bed conditions. For d_{84} , $C_1 = 5.09$ and $C_2 = 1.23$ were obtained, as were $C_1 = 5.46$ and $C_2 = 1.25$ for d_{90} , which rules out the possibility of attributing the difference between the fitted values and those proposed by Katul *et al.* (2002) to the inclusion of data with high relative submergence or mobile bed. The same trend was observed in López *et al.* (2006) for the analysis described above.

Given that the subset of river data represented 62% of the total database, the coefficients obtained on fitting the models to the whole database (Table 3) were closer to those obtained from the subset of river data (Tables 4 and 5). However, these tables show that the difference between the river and flume equations in the value of the fitted coefficients is much lower for models fitted to d_{90} than for those fitted to d_{50} . In fact, the mean of the difference of all coefficients reached 67% for d_{50} , while it was only 13% for d_{90} . The greater disparity for d_{50} was also detected by Ferro and Giordano (1991) on comparing logarithmic equations (model (3)) fitted to databases that differed in the concentration of coarser elements.

On the other hand, from value of the fitted coefficients shown in Tables 4 and 5 it follows that, for the same relative submergence, the equation fitted to the river database predicts higher flow resistance (i.e., a higher value of f) than the equation fitted to the flume database. This would mainly be explained by the lower

Table 5. Coefficients and statistics of the models fitted separately to the river and flume databases. Grain-size percentile: d_{90} .

| Model | Eq. | Database | Coefficients | R^2 | MRE (%) | RE ₂₅ (%) | RE ₅₀ (%) |
|-------|------|----------|---------------------------|-------|---------|----------------------|----------------------|
| (3) | (21) | River | $A_1 = 5.67; A_2 = 4.02$ | 0.73 | 27 | 61 | 87 |
| (3) | (22) | Flume | $A_1 = 5.92; A_2 = 4.59$ | 0.82 | 16 | 83 | 94 |
| (4) | (23) | River | $B_1 = 2.72; B_2 = 0.111$ | 0.72 | 26 | 61 | 88 |
| (4) | (24) | Flume | $B_1 = 2.79; B_2 = 0.089$ | 0.81 | 16 | 82 | 94 |
| (5) | (25) | River | $C_1 = 5.71; C_2 = 1.20$ | 0.73 | 30 | 64 | 87 |
| (5) | (26) | Flume | $C_1 = 6.12; C_2 = 1.53$ | 0.80 | 17 | 82 | 93 |

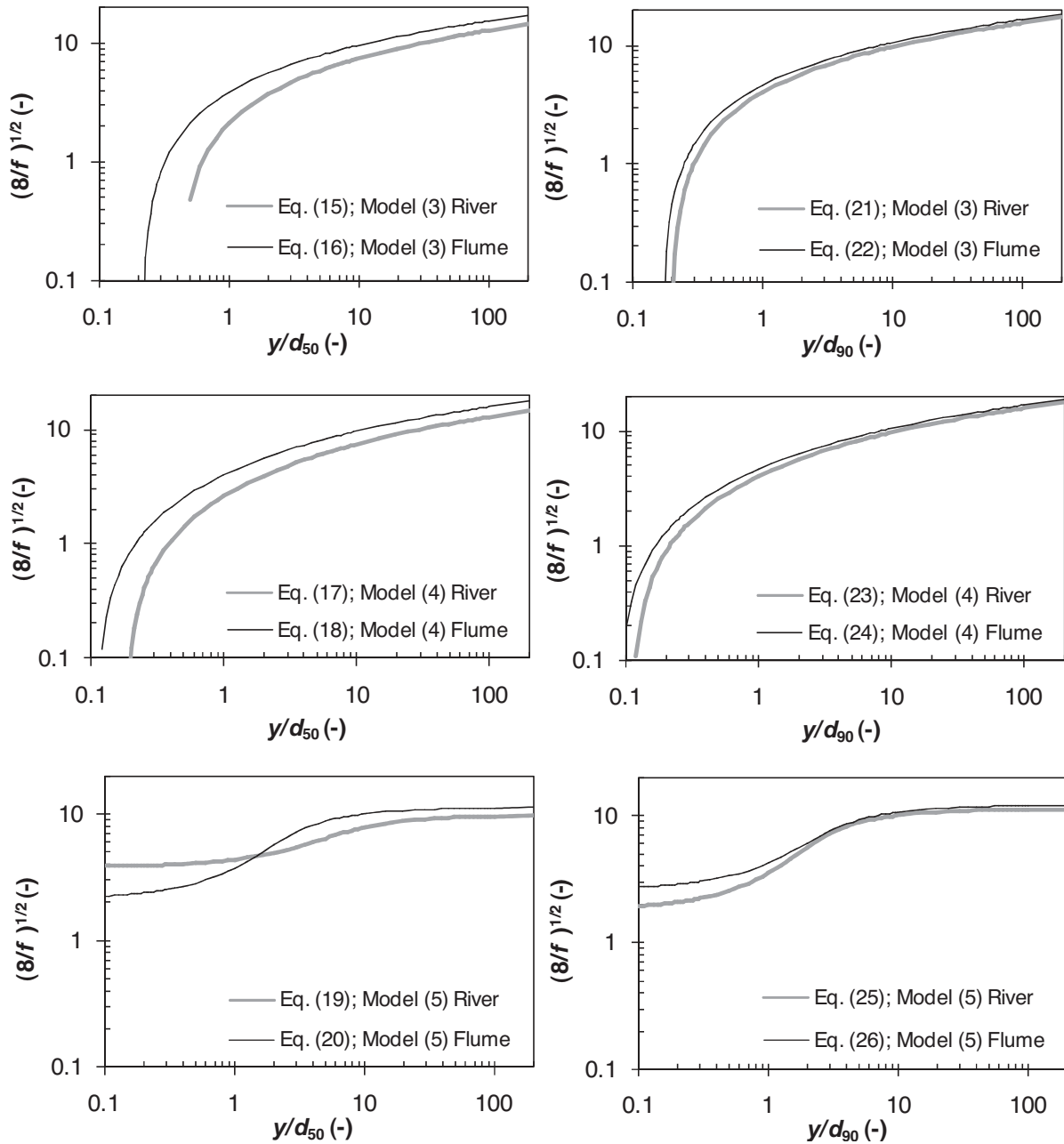


Figure 4. Representation of the equations fitted separately to the data subsets for rivers and flumes.

degree of compliance with the prismatic and straight channel hypotheses by the river data and the lower proportion of flume data with bedforms (on both large and small scales), differences that provoke a higher energy loss in the river reaches. Similarly, Tables 4 and 5 shows the higher explanatory power of the equations fitted to the flume database compared to those fitted to the river database. This should be attributed mainly to the greater

difficulty and poorer measurement conditions in coarse material-bed rivers compared with flumes, to the deviations from the prismatic character in the river reaches and to the contribution of sinuosity, although this last factor of limited significance.

The mean values of the statistical indices resulting from the crossed validation of equations (8), (11) and (14), to both validation sets (Table 6), were practically

Table 6. Statistics corresponding to the cross validation of equations (8), (11) and (14)

| Model | Eq. | R^2 | MRE (%) | RE ₂₅ (%) | RE ₅₀ (%) |
|-------|------|-------|---------|----------------------|----------------------|
| (3) | (8) | 0.76 | 24 | 69 | 88 |
| (4) | (11) | 0.76 | 24 | 68 | 89 |
| (5) | (14) | 0.76 | 26 | 69 | 89 |

identical to those obtained in the regression phase were obtained for the three models, which supports the precision of the explanatory power of the fitted models when they are applied to data not included in the calibration.

Conclusions

The conclusions presented below were obtained from the evaluation of the flow resistance logarithmic model and the two other models developed for flows with high relative roughness conditions. A large database ($N = 1,533$) was used, representative of a wide hydraulic and geomorphological range of gravel-bed and mountain channels.

Higher explanatory power and lower fitting error were achieved by fitting the models to the coarser percentiles, d_{90} or d_{84} , than to the median diameter d_{50} . Furthermore, a higher difference was observed in the goodness-of-fit of the three models when these were fitted to the median diameter rather than to the coarser percentiles. On the other hand, fitting the models separately to river and flume data led to a higher difference in the value of the coefficients when d_{50} was used instead of d_{90} . For all these reasons, models fitted to d_{90} or d_{84} are preferable to those fitted to the median diameter d_{50} .

For the equations derived separately for river and flume data, there are no important differences in the value of the fitted coefficients if the coarser percentiles are used. However, the models fitted to the river data predict a slightly higher flow resistance and show lesser explanatory power. This is attributable to the lower degree of compliance with the experimental restrictions imposed (geomorphological and hydraulic homogeneity) and the fact that the measurement errors are larger in rivers.

It follows from this discussion that, among the different fitted models in this study, equations (8), (11) and (14) are most recommended. Equation (14), based on an inflectional velocity profile, is preferable for application in the y/d_{90} interval between 0.5 and 15, while

equation (11), based on the full logarithmic equation, is preferable for values below 0.5. For relative submergence exceeding 15, either equations (8) or (11) can be used.

References

- ABERLE J., SMART G.M., 2003. The influence of roughness structure on flow resistance on steep slopes. *J. Hydraul. Res.* 41(3), 259–269.
- AGUIRRE-PE J., FUENTES R., 1990. Resistance to flow in steep rough streams. *J. Hydraul. Eng.* 116(11), 1374–1386.
- BATHURST J.C., 1985. Flow resistance estimation in mountain rivers. *J. Hydraul. Eng.* 111(4), 625–643.
- BRAY D.I., 1979. Estimating average velocity in gravel-bed rivers. *J. Hydraul. Div., Am. Soc. Civ. Eng.* 105(9), 1103–1122.
- BURKHAM D.E., DAWDY, D.R., 1976. Resistance equation for alluvial-channel flow. *J. Hydraul. Div., Am. Soc. Civ. Eng.* 102(10), 1479–1489.
- CHARLTON F.G., BROWN P.M., BENSON, R.W., 1978. The hydraulic geometry of some gravel rivers in Britain. Report N° IT 180. Hydraulics Research Station. Wallingford, UK.
- CLIFFORD N.J., ROBERT A., RICHARDS, K.S., 1992. Estimation of flow resistance in gravel-bedded rivers: a physical explanation of the multiplier of roughness length. *Earth Surf. Process. Landforms* 17, 111–126.
- ESBENSEN K., SCHÖNKOPF S., MIDTGAARD T., 1994. Multivariate analysis in practice. CAMO AS. Trondheim, Norway, 312 pp.
- FERGUSON R., 2007. Flow resistance equations for gravel- and boulder-bed streams. *Water Resour. Res.* 43, W05427.
- FERRO V., GIORDANO, G., 1991. Experimental study of flow resistance in gravel-bed rivers. *J. Hydraul. Eng.* 117(10), 1239–1246.
- GREEN J.C., 2003. The precision of sampling grain-size percentiles using the Wolman method. *Earth Surf. Process. Landforms* 28(9), 979–991.
- GREEN J.C., 2005. Choice of percentiles and axes to determine grain resistance. *J. Hydraul. Eng.* 131(11), 1007–1010.
- GRIFFITHS G.A., 1981. Flow resistance in coarse gravel bed rivers. *J. Hydraul. Div., Am. Soc. Civ. Eng.* 107(7), 899–918.
- KATUL G., WIBERG P., ALBERTSON J., HORNBERGER G., 2002. A mixing layer theory for flow resistance in shallow streams. *Water Resour. Res.* 38(11), 1250.
- KNIGHTON D., 1998. Fluvial forms and processes: A new perspective. Arnold. London, UK, 383 pp.

- LIMERINOS J.T., 1970. Determination of the Manning coefficient from measured bed roughness in natural channels. Water Supply Paper 1898-B. U.S. Geological Survey. Washington.
- LÓPEZ R., 2005. Resistencia al flujo de ríos de montaña: Desarrollo de ecuaciones de predicción. Tesis doctoral. Universidad de Lleida.
- LÓPEZ R., BARRAGÁN J., COLOMER M.A., 2006. Evaluación de ecuaciones de resistencia al flujo sobre escollera. Ingeniería del Agua 13(2), 99–111.
- LÓPEZ R., BARRAGÁN J., COLOMER M.A., 2008. Predicción de la resistencia al flujo en ríos de montaña. Ingeniería Hidráulica en México XXIII(3), 67–78.
- MAYNORD S., 1991. Flow resistance of riprap. J. Hydraul. Eng. 117(6), 687–696.
- PRESTEGAARD K.L., 1983. Bar resistance in gravel bed streams at bankfull stage. Water Resour. Res. 19(2), 472–476.
- RICE S., CHURCH M., 1996. Sampling surficial fluvial gravels: the precision of size distribution percentile estimates. J. Sedimentary Res. 66(3), 654–665.
- SMART G.M., 1984. Sediment transport formula for steep channels. J. Hydraul. Eng. 110(3), 267–276.
- SMART G.M., DUNCAN M.J., WALSH, J.M., 2002. Relatively rough flow resistance equations. J. Hydraul. Eng. 128(6), 568–578.
- THOMPSON S.M., CAMPBELL P.L., 1979. Hydraulics of a large channel paved with boulders. J. Hydraul. Res. 17(4), 341–354.
- UGARTE A., MÉNDEZ, R., 1994. Resistencia al flujo en ríos de montaña. Actas del XVI Congreso Latinoamericano de Hidráulica, Santiago, Chile, pp. 503–514.
- VAN RIJN L.C., 1982. Equivalent roughness of alluvial bed. J. Hydraul. Div., Am. Soc. Civ. Eng. 108(10), 1215–1218.
- WHITING P.J., DIETRICH W.E., 1990. Boundary shear stress and roughness over mobile alluvial beds. J. Hydraul. Eng. 116(12), 1495–1511.

Notation

- d_i = particle size of percentile i
 f = Darcy-Weisbach friction factor
 g = gravitational acceleration
 h = flow depth
 k_s = equivalent roughness
 R = hydraulic radius
 Re = Reynolds number
 Re_* = grain shear Reynolds number
 S = bed slope
 V = mean velocity
 v_* = shear velocity
 y = mean flow depth
 z_0 = hydraulic roughness of the boundary
 κ = von Karman coefficient
 ν = kinematic viscosity of water
 τ = mean shear stress
 τ_c = critical shear stress